Journal of Theoretical and Applied Mechanics, Sofia, Vol.52 (2022) pp. 103-117
SOLID MECHANICS

AXIAL BUCKLING ANALYSIS OF FUNCTIONALLY GRADED PLATES (AL/AL_2O_3) USING NAVIER METHOD

BOUDERBA BACHIR[1], BERRABAH HAMZA MADJID[1*]

[1]*Department of Science and Technology, Mechanical Engineering Materials and Structures Laboratory, Ahmed Ben Yahia Al-Wancharissi University – Tissemsilt, Tissemsilt, Algeria*
[2]*Department of Civil Engineering, Mechanical Engineering Materials and Structures Laboratory, Ahmed Zabana University – Relizane, Relizane, Algeria*

[Received: 17 December 2020. Accepted: 05 April 2021]

doi: https://doi.org/10.55787/jtams.22.52.2.103

ABSTRACT: In the present paper, exact solution of the axial buckling analysis to the functionally graded materials plates (Al/Al_2O_3) is studied. Using a four variable refined plate theory, both a quadratic variation of the transverse shear strains across the thickness and the zero traction boundary conditions on the top and bottom surfaces of the plate is satisfied without using shear correction factors, from the principle of minimum total potential energy, we obtain the governing equations. The number of independent unknowns of present theory is four, as against five in other shear deformation theories. Numerical examples on the buckling analysis of functionally graded plate demonstrate the accuracy of the present approach.

KEY WORDS: axial, buckling, shear, strains, deformation, FGP.

1 INTRODUCTION

Composite structures have long been of vivid interest to researchers because it is an undesired phenomenon and some cases of it cannot be avoided under special conditions. Recently, advanced composite materials known as functionally graded material have attracted much attention in many engineering applications due to their advantages of being able to resist high temperature gradient while maintaining structural integrity [1]. The functionally graded materials (FGMs) are microscopically inhomogeneous, in which the mechanical properties vary smoothly and continuously from one surface to the other. The classical Kirchhoff plate theory neglects transverse shear deformation and gives acceptable results for relatively thin plates. In order to

*Corresponding author e-mail: b_hamza_2005@yahoo.fr

circumvent this problem earlier attempts were made by Reissner [2] and Mindlin [3]. However, a shear correction factor must be incorporated to overcome the problem of a constant transverse shear stress distribution and its value depends on various parameters, such as applied loads, boundary conditions and geometric parameters, etc. The inaccuracy occurs due to neglecting the effects of transverse shear and normal strains in the plate [4]. Due to continuous variation in material properties, the first-order shear deformation theory and higher order shear deformation theory may be conveniently used in the analysis. It is noted that the first-order shear deformation theory proposed by Mindlin [3] does not satisfy the parabolic variation of transverse shear strain in the thickness direction. Subsequently, many higher order theories were proposed, notable among them are [5–8]. The higher order theories assume the in-plane displacements as a cubic expression of the thickness coordinate and the out-of-plane displacement to be constant. Thus, the development of higher order shear deformation theory to assimilate the behaviour of FGM structures has been of high importance to the researchers. In the literature, studies of the buckling of FGM structures are as follows, several researchers have studied different phenomena such as buckling analysis of FGM plates under uniform, linear and non-linear in-plane loading is studied by [9]. In this paper, an efficient and simple refined theory is presented for buckling analysis of functionally graded thick plates. Numerical examples cover the effects of the gradient index, plate aspect ratio, side-to-thickness ratio on the critical buckling load of functionally graded plates are investigated and discussed. The buckling response of plates with functional gradation is presented in this article using Navier's method with plate theory with four variables. The properties of the materials of the plate are supposed to vary according to a form of power law in the direction of thickness. Equilibrium equations are calculated analytically.

2 Formulation

Consider a functionally graded plate of thickness$h$, side length a in x-direction, and b in y-direction as shown in Fig. 1.

The assumptions of the present theory are as follows (see Shimpi [10]):

— the transverse displacements are partitioned into bending and shear components;

— the in-plane displacement is partitioned into extension, bending, and shears components;

— the bending parts of the in-plane displacements are similar to those given by classical plate theory (CPT);

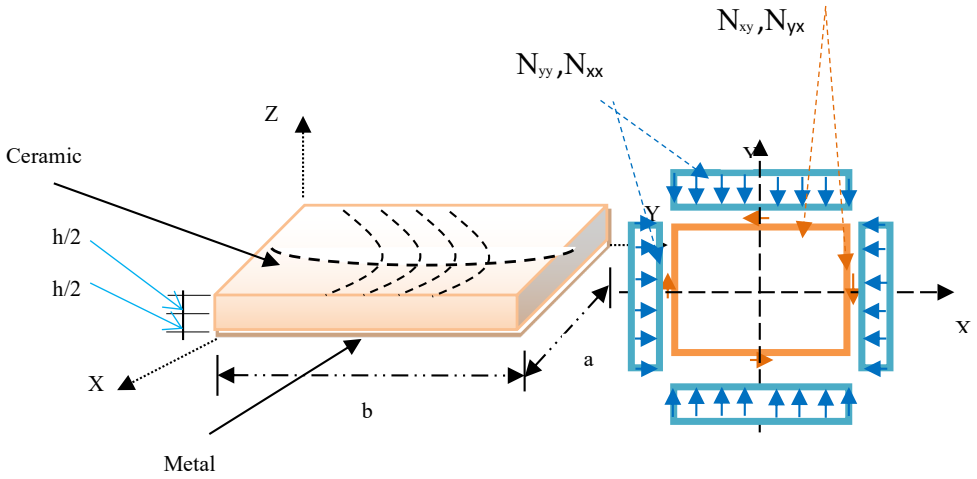

Fig. 1: Geometry for rectangular FG plate subjected to compressive in-plane forces and distributed shear forces.

— the shear parts of the in-plane displacements give rise to the nonlinear variations of shear strains and hence to shear stresses through the thickness of the plate in such a way that the shear stresses vanish on the top and bottom surfaces of the plate.

Based on these assumptions, the following displacement field relations can be obtained:

$$
\begin{aligned}
U(x,y,z) &= u(x,y) - z\frac{\partial w_b}{\partial x} - \xi(z)\frac{\partial w_s}{\partial x}\,,\\
V(x,y,z) &= v(x,y) - z\frac{\partial w_b}{\partial y} - \xi(z)\frac{\partial w_s}{\partial y}\,,\\
W(x,y,z) &= w_b(x,y) + w_s(x,y)\,,
\end{aligned}
\tag{1}
$$

where U, V, W are displacements in the x, y, z directions, u, v and w_b, w_s are mid-plane displacements and $\xi(z)$ is a shape function that represents the distribution of the transverse shear strain and stress through the thickness, as presented in Table 1.

Consider a FG plate made of ceramic and metal, the material properties of FGM such as Young's modulus E are assumed to vary through the plate thickness with a power law distribution of the volume fraction of the two materials

$$
E(z) = (E_{cm})V_C(z) + E_m\,, \quad E_{cm} = E_c - E_m\,,
\tag{2}
$$

where E_c and E_m are the corresponding properties of the ceramic and metal, respectively, and p is the volume fraction exponent which takes values greater than or equal

Table 1: Different shear stress function

Model	$\xi(z)$ function
Ambartsumian [11]	$\xi(z) = (z/2)(h^2/4 - z^2/3)$
Karama et al. [12] and Aydogdu [13]	$\xi(z) = ze^{-2(z/h)^2}$
Kaczkowski [14], Panc [15], Reissner [6]	$\xi(z) = (5z/4)(1 - 4z^2/(3h^2))$
Tounsi et al. [16], Bouderba et al. [17]	$\xi(z) = z - (h/\pi)\sin(\pi z/h)$
Levinson [18], Murthy [19] and Reddy [20]	$\xi(z) = z(1 - 4z^2/(3h^2))$
Sobhy [21]	$\xi(z) = z/(1 + 4z^2/h^2)$
Touratier [22]	$\xi(z) = (h/\pi)\sin(\pi z/h)$
Soldatos [23]	$\xi(z) = h\sinh(z/h) - z\cosh(1/2)$
Present	$\xi(z) = z - z/(1 + 4z^2/h^2)$

to zero. The volume fraction V_C (z) follows a simple power law as [24]:

1. Linear: $V_C(z) = (z/h + 0.5)^p$;
2. Quadratic: $V_C(z) = ((z/h + 0.5)^2)^p$;
3. Cubic: $V_C(z) = (3(z/h + 0.5)^2 - 2(z/h + 0.5)^3)^p$;
4. Inverse quadratic: $V_C(z) = (1 - (0.5 - z/h)^2)^p$.

The kinematic relations can be obtained as follows:

$$(3)\quad \begin{Bmatrix} \varepsilon_x \\ \varepsilon_y \\ \gamma_{xy} \end{Bmatrix} = \begin{Bmatrix} \varepsilon_x^0 \\ \varepsilon_y^0 \\ \gamma_{xy}^0 \end{Bmatrix} + z \begin{Bmatrix} k_x^b \\ k_y^b \\ k_{xy}^b \end{Bmatrix} + \xi(z) \begin{Bmatrix} k_x^s \\ k_y^s \\ k_{xy}^s \end{Bmatrix}, \quad \begin{Bmatrix} \gamma_{yz} \\ \gamma_{xz} \end{Bmatrix} = g(z) \begin{Bmatrix} \gamma_{yz}^s \\ \gamma_{xz}^s \end{Bmatrix},$$

where

$$\begin{Bmatrix} \varepsilon_x^0 \\ \varepsilon_y^0 \\ \gamma_{xy}^0 \end{Bmatrix} = \begin{Bmatrix} \partial u/\partial x \\ \partial v/\partial y \\ \partial u/\partial y + \partial v/\partial x \end{Bmatrix}, \qquad \begin{Bmatrix} k_x^b \\ k_y^b \\ k_{xy}^b \end{Bmatrix} = \begin{Bmatrix} -\partial^2 w_b/\partial x^2 \\ -\partial^2 w_b/\partial y^2 \\ -2\partial^2 w_b/\partial x \partial y \end{Bmatrix},$$

$$\begin{Bmatrix} k_x^s \\ k_y^s \\ k_{xy}^s \end{Bmatrix} = \begin{Bmatrix} -\partial^2 w_s/\partial x^2 \\ -\partial^2 w_s/\partial y^2 \\ -2\partial^2 w_s/\partial x \partial y \end{Bmatrix}, \qquad \begin{Bmatrix} \gamma_{yz}^s \\ \gamma_{xz}^s \end{Bmatrix} = \begin{Bmatrix} \partial w_s/\partial y \\ \partial w_s/\partial x \end{Bmatrix}$$

and $\xi(z)$ given by:

$$(4)\qquad \xi(z) = z - \left(\frac{z}{1 + 4z^2/h^2}\right), \qquad g(z) = 1 - \frac{d\xi(z)}{dz}.$$

The linear constitutive relations are

$$(5)\quad \begin{Bmatrix}\sigma_x\\ \sigma_y\\ \tau_{xy}\end{Bmatrix} = \begin{bmatrix}Q_{11} & Q_{12} & 0\\ Q_{12} & Q_{22} & 0\\ 0 & 0 & Q_{66}\end{bmatrix}\begin{Bmatrix}\varepsilon_x\\ \varepsilon_y\\ \gamma_{xy}\end{Bmatrix} \text{ and } \begin{Bmatrix}\tau_{yz}\\ \tau_{zx}\end{Bmatrix} = \begin{bmatrix}Q_{44} & 0\\ 0 & Q_{55}\end{bmatrix}\begin{Bmatrix}\gamma_{yz}\\ \gamma_{zx}\end{Bmatrix},$$

where $(\sigma_x,\ \sigma_y,\ \tau_{xy},\ \tau_{yz},\ \tau_{yx})$ and $(\varepsilon_x,\ \varepsilon_y,\ \gamma_{xy},\ \gamma_{yz},\ \gamma_{yx})$ are the stress and strain components, respectively. Stiffness coefficients, Q_{ij}, can be expressed as

$$(6)\quad Q_{11} = Q_{22} = \frac{E(z)}{1-\nu^2}, \quad Q_{12} = \frac{\nu E(z)}{1-\nu^2}, \quad Q_{44} = Q_{55} = Q_{66} = \frac{E(z)}{2(1+\nu)}.$$

The strain energy of the plate can be written

$$(7)\qquad U = \frac{1}{2}\int_V [\sigma_x\varepsilon_x + \sigma_y\varepsilon_y + \tau_{xy}\gamma_{xy} + \tau_{yz}\gamma_{yz} + \tau_{zx}\gamma_{zx}]dV\,.$$

Substituting Eqs. (3) and (5) into Eq. (7) and integrating through the thickness of the plate, the strain energy of the plate can be rewritten as

$$(8)\quad U = \frac{1}{2}\int_A \big[N_x\varepsilon_x^0 + N_y\varepsilon_y^0 + N_{xy}\varepsilon_{xy}^0 + M_x^b k_x^b + M_y^b k_y^b + M_{xy}^b k_{xy}^b + M_x^s k_x^s + M_y^s k_y^s + M_{xy}^s k_{xy}^s + S_{yz}^s\gamma_{yz}^s + S_{xz}^s\gamma_{xz}^s\big]dxdy\,,$$

where the resultants forces, moments and shear forces, which are all defined by

$$(9)\quad \begin{aligned}(N_x, N_y, N_{xy}) &= \int_{-h/2}^{h/2}(\sigma_x,\sigma_y,\tau_{xy})dz\,,\\ (M_x^b, M_y^b, M_{xy}^b) &= \int_{-h/2}^{h/2}(\sigma_x,\sigma_y,\tau_{xy})z dz\,,\\ (M_x^s, M_y^s, M_{xy}^s) &= \int_{-h/2}^{h/2}(\sigma_x,\sigma_y,\tau_{xy})\xi dz\,,\\ (S_{xz}^s, S_{yz}^s) &= \int_{-h/2}^{h/2}(\sigma_x,\sigma_y,\tau_{xy})g dz\,.\end{aligned}$$

Substituting Eq. (5) into Eq. (9) and integrating through the thickness of the plate, the stress resultants are given as

$$(10)\quad \begin{Bmatrix} N \\ M^b \\ M^s \end{Bmatrix} = \begin{bmatrix} A & B & B^s \\ B & D & D^s \\ B^s & D^s & H^s \end{bmatrix} \begin{Bmatrix} \varepsilon \\ k^b \\ k^s \end{Bmatrix}, \quad \begin{Bmatrix} S^s_{yz} \\ S^s_{xz} \end{Bmatrix} = \begin{bmatrix} A^s_{44} & 0 \\ 0 & A^s_{55} \end{bmatrix} \begin{Bmatrix} \gamma^s_{yz} \\ \gamma^s_{xz} \end{Bmatrix},$$

where

$$(11)\quad N=\{N_x, N_y, N_{xy}\}^t, \qquad M^b=\{M^b_x, M^b_y, M^b_{xy}\}^t, \quad M^s=\{M^s_x, M^s_y, M^s_{xy}\}^t,$$

$$(12)\quad \varepsilon = \{\varepsilon^0_x, \varepsilon^0_y, \gamma^0_{xy}\}, \qquad k^b = \{k^b_x, k^b_y, k^b_{xy}\},$$

$$(13)\quad A=\begin{bmatrix} A_{11} & A_{12} & 0 \\ A_{12} & A_{22} & 0 \\ 0 & 0 & A_{66} \end{bmatrix}, \quad B=\begin{bmatrix} B_{11} & B_{12} & 0 \\ B_{12} & B_{22} & 0 \\ 0 & 0 & B_{66} \end{bmatrix}, \quad D=\begin{bmatrix} D_{11} & D_{12} & 0 \\ D_{12} & D_{22} & 0 \\ 0 & 0 & D_{66} \end{bmatrix},$$

$$(14)\quad B^s = \begin{bmatrix} B^s_{11} & B^s_{12} & 0 \\ B^s_{12} & B^s_{22} & 0 \\ 0 & 0 & B^s_{66} \end{bmatrix}, D^s = \begin{bmatrix} D^s_{11} & D^s_{12} & 0 \\ D^s_{12} & D^s_{22} & 0 \\ 0 & 0 & D^s_{66} \end{bmatrix}, H^s = \begin{bmatrix} H^s_{11} & H^s_{12} & 0 \\ H^s_{12} & H^s_{22} & 0 \\ 0 & 0 & H^s_{66} \end{bmatrix},$$

where A_{ij}, B_{ij}, etc., are the plate stiffness defined by

$$(15)\quad \{A_{ij}, B_{ij}, D_{ij}, E_{ij}, F_{ij}, H_{ij}\} = \int_{-h/2}^{+h/2} \{1, z, z^2, z^3, z^4, z^6\} Q_{ij} dz \quad (i,j=1,2,6),$$

$$B^s_{ij} = -\frac{1}{4}B_{ij} + \frac{5}{3h^2}E_{ij} \qquad (i,j=1,2,6),$$

$$D^s_{ij} = -\frac{1}{4}D_{ij} + \frac{5}{3h^2}F_{ij} \qquad (i,j=1,2,6),$$

$$H^s_{ij} = \frac{1}{16}D_{ij} - \frac{5}{6h^2}F_{ij} + \frac{25}{9h^4}H_{ij} \qquad (i,j=1,2,6)$$

$$(16)\quad \{A_{ij}, D_{ij}, F_{ij}\} = \int_{-h/2}^{+h/2} \{1, z^2, z^4\} Q_{ij} dz \qquad (i,j=4,5)$$

$$A^s_{ij} = \frac{25}{16}A_{ij} - \frac{25}{6h^2}D_{ij} + \frac{25}{h^4}F_{ij} \qquad (i,j=4,5).$$

The work done by applied forces can be written as

$$V = \frac{1}{2}\int_A N_x^0\Big(\frac{\partial(w_b+w_s)}{\partial x}\Big)^2 + N_y^0\Big(\frac{\partial(w_b+w_s)}{\partial y}\Big)^2 + 2N_{xy}^0\frac{\partial(w_b+w_s)}{\partial x}\frac{\partial(w_b+w_s)}{\partial y}dxdy\,, \tag{17}$$

where N_x^0, N_y^0, N_{xy}^0 are in-plane pre-buckling forces.

The governing equations of equilibrium can be obtained as follows:

$$\begin{aligned}
&\delta u : \frac{\partial N_x}{\partial x} + \frac{\partial N_{xy}}{\partial y} = 0\,, \quad \delta v : \frac{\partial N_{xy}}{\partial x} + \frac{\partial N_y}{\partial y} = 0\,,\\
&\delta w_b : \frac{\partial^2 M_x^b}{\partial x^2} + 2\frac{\partial^2 M_{xy}^b}{\partial x\partial y} + \frac{\partial^2 M_y^b}{\partial y^2} + P(w) = 0\,,\\
&\delta w_s : \frac{\partial^2 M_x^s}{\partial x^2} + 2\frac{\partial^2 M_{xy}^s}{\partial x\partial y} + \frac{\partial^2 M_y^s}{\partial y^2} + \frac{\partial S_{xz}^s}{\partial x} + \frac{\partial S_{yz}^s}{\partial y} + P(w) = 0\,,
\end{aligned} \tag{18}$$

where

$$P(w) = N_x^0\frac{\partial^2(w_b+w_s)}{\partial x^2} + N_y^0\frac{\partial^2(w_b+w_s)}{\partial y^2} + 2N_{xy}^0\frac{\partial^2(w_b+w_s)}{\partial x\partial y}\,. \tag{19}$$

Substituting from Eq. (6) into Eq. (13), we obtain the following equation:

$$\begin{aligned}
&A_{11}d_{11}u + A_{66}d_{22}u + (A_{12}+A_{66})d_{12}v - B_{11}d_{111}w_b\\
&\quad - (B_{12}+2B_{66})d_{122}w_b - (B_{12}^s+2B_{66}^s)d_{122}w_s - B_{11}^s d_{111}w_s = 0\,,\\
&A_{22}d_{22}v + A_{66}d_{11}v + (A_{12}+A_{66})d_{12}u - B_{22}d_{222}w_b\\
&\quad - (B_{12}+2B_{66})d_{112}w_b - (B_{12}^s+2B_{66}^s)d_{112}w_s - B_{22}^s d_{222}w_s = 0\,,\\
&B_{11}d_{111}u + (B_{12}+2B_{66})d_{122}u + (B_{12}+2B_{66})d_{112}v\\
&\quad + B_{22}d_{222}v - D_{11}d_{1111}w_b - 2(D_{12}+2D_{66})d_{1122}w_b - D_{22}d_{2222}w_b\\
&\quad - D_{11}^s d_{1111}w_s - 2(D_{12}^s+2D_{66}^s)d_{1122}w_s - D_{22}^s d_{2222}w_s + P(w) = 0\,,\\
&B_{11}^s d_{111}u + (B_{12}^s+2B_{66}^s)d_{122}u + (B_{12}^s+2B_{66}^s)d_{112}v + B_{22}^s d_{222}v\\
&\quad - D_{11}^s d_{1111}w_b - 2(D_{12}^s+2D_{66}^s)d_{1122}w_b - D_{22}^s d_{2222}w_b - H_{11}^s d_{1111}w_s\\
&\quad - 2(H_{12}^s+2H_{66}^s)d_{1122}w_s - H_{22}^s d_{2222}w_s + A_{55}^s d_{11}w_s\\
&\quad + A_{44}^s d_{22}w_s + P(w) = 0\,,
\end{aligned} \tag{20}$$

where d_{ij}, d_{ijl} and d_{ijlm} are the following differential operators:

$$\begin{aligned}
&d_{ij} = \frac{\partial^2}{\partial x_i\partial x_j}\,, \qquad d_{ijl} = \frac{\partial^3}{\partial x_i\partial x_j\partial x_l}\,,\\
&d_{ijlm} = \frac{\partial^4}{\partial x_i\partial x_j\partial x_l\partial x_m}\,, \quad d_i = \frac{\partial}{\partial x_i}\,, \quad (i,j,l,m=1,2).
\end{aligned} \tag{21}$$

Consider a simply supported rectangular plate with length a and width b which is subjected to in-pline loading in two directions ($N_x^0 = \gamma_1 N_{cr}$, $N_y^0 = \gamma_2 N_{cr}$, $N_{xy}^0 = 0$). Based on the Navier method, the following expansions of displacements (u, v, w_b, w_s):

$$\begin{Bmatrix} u \\ v \\ w_b \\ w_s \end{Bmatrix} = \sum_{m=1}^{\infty}\sum_{n=1}^{\infty} \begin{Bmatrix} U_{mn}\cos(\lambda x)\sin(\mu y) \\ V_{mn}\sin(\lambda x)\cos(\mu y) \\ W_{bmn}\sin(\lambda x)\sin(\mu y) \\ W_{smn}\sin(\lambda x)\sin(\mu y) \end{Bmatrix}, \tag{22}$$

where $\lambda = m\pi/a$, $\mu = n\pi/b$, and $(U_{mn}, V_{mn}, W_{bmn}, W_{smn})$ are unknown functions to be determined. Substituting Eq. (16) into Eq. (15), the closed-form solution of buckling load N_{cr} can be obtained from

$$\begin{bmatrix} \Theta_{11} & \Theta_{12} & \Theta_{13} & \Theta_{14} \\ \Theta_{12} & \Theta_{22} & \Theta_{23} & \Theta_{24} \\ \Theta_{13} & \Theta_{23} & \Theta_{33}+K & \Theta_{34}+K \\ \Theta_{14} & \Theta_{24} & \Theta_{34}+K & \Theta_{44}+K \end{bmatrix} \begin{Bmatrix} U_{mn} \\ V_{mn} \\ W_{bmn} \\ W_{smn} \end{Bmatrix} = \begin{Bmatrix} 0 \\ 0 \\ 0 \\ 0 \end{Bmatrix}, \tag{23}$$

where

$$\begin{aligned}
\Theta_{11} &= A_{11}\lambda^2 + A_{66}\mu^2\,, \\
\Theta_{12} &= \lambda\mu(A_{12} + A_{66}), \\
\Theta_{13} &= -\lambda[B_{11}\lambda^2 + (B_{12} + 2B_{66})\mu^2], \\
\Theta_{14} &= -\lambda[B_{11}^s\lambda^2 + (B_{12}^s + 2B_{66}^s)\mu^2], \\
\Theta_{22} &= A_{66}\lambda^2 + A_{22}\mu^2, \\
\Theta_{23} &= -\mu[(B_{12} + 2B_{66})\lambda^2 + B_{22}\mu^2], \\
\Theta_{24} &= -\mu[(B_{12}^s + 2B_{66}^s)\lambda^2 + B_{22}^s\mu^2], \\
\Theta_{33} &= D_{11}\lambda^4 + 2(D_{12} + 2D_{66})\lambda^2\mu^2 + D_{22}\mu^4, \\
\Theta_{34} &= D_{11}^s\lambda^4 + 2(D_{12}^s + 2D_{66}^s)\lambda^2\mu^2 + D_{22}^s\mu^4, \\
\Theta_{44} &= H_{11}^s\lambda^4 + 2(H_{11}^s + 2H_{66}^s)\lambda^2\mu^2 + H_{22}^s\mu^4 + A_{55}^s\lambda^2 + A_{44}^s\mu^2 \\
K &= N_{cr}(\gamma_1\lambda^2 + \gamma_2\mu^2).
\end{aligned} \tag{24}$$

The nondimensional critical buckling load is defined as

$$\bar{N} = N_{cr}a^2/E_m h^3\,. \tag{25}$$

Functionally graded rectangular plate which its mechanical properties vary smoothly and continuously along the thickness direction from one surface to the other. The variation of Poisson's ratio is generally small and it is assumed to be a constant for convenience, see: [21, 24, 25].

3 Numerical Results and Discussions

For having a numerical study and investigation, it is assumed that FGM plate is made of Alumina (Al_2O_3) as the ceramic part ($E_c = 380$ GPa) and aluminum (Al) as metal part ($E_m = 70$ GPa). Also, the Poisson ratio is constant and equal to $v = 0.3$.

Table 2 shows the comparisons of the critical buckling loads obtained by the present theory with those given by [25] based on CPT, Shariat and Eslami [26] based on FSDT, and Bodaghi and Saidi [27] based on HSDT, Thai and Choi [28] based on RPSDT. It can be seen that the results of present theory are in excellent agreement with those obtained by HSDT [27] for all values of thickness ratio a/h. It should be noted that the present theory involves only four independent variables as against five in the case of HSDT [27] and FSDT [26]. Also, the present theory does not require shear correction factors as in the case of FSDT. It can be concluded that the present theory is not only accurate but also efficient in predicting critical buckling load of FG plates.

Table 2: Critical buckling load of simply supported FGM (Al/Al_2O_3) plate ($a/b = 0.5, p = 1$)

(γ_1, γ_2)	Theory	a/h					
		5	10	20	30	40	50
(-1,0)	CPT [25]	267.4800	33.4350	4.1794	1.2383	0.5224	0.2675
	FSDT [26]	243.4100	32.6280	4.1537	1.2349	0.5216	0.2672
	HSDT [27]	239.1500	32.4720	4.1486	1.2343	0.5215	0.2672
	RPSDT [28]	239.1450	32.4721	4.1486	1.2343	0.5215	0.2672
	Present	239.1450	32.4721	4.1486	1.2343	0.5215	0.2672
(-1,-1)	CPT [25]	213.9900	26.7480	3.4353	0.9907	0.4179	0.2140
	FSDT [26]	194.7300	26.1030	3.3230	0.9880	0.4173	0.2137
	HSDT [27]	191.3200	25.9780	3.3189	0.9879	0.4172	0.2137
	RPSDT [28]	191.3160	25.9777	3.3189	0.9874	0.4172	0.2137
	Present	191.3160	25.9777	3.3189	0.9874	0.4172	0.2137
(-1,1)	CPT [25]	356.6400	44.5800	5.5725	1.6511	0.6966	0.3566
	FSDT [26]	324.5400	43.5050	5.5383	1.6466	0.6955	0.3563
	HSDT [27]	318.8600	43.2960	5.5315	1.6457	0.6953	0.3562
	RPSDT [28]	318.8600	43.2961	5.5315	1.6457	0.6953	0.3562
	Present	318.8601	43.2961	5.5315	1.6457	0.6953	0.3562

The variation of nondimensional critical buckling load of plate versus thickness ratio a/h is demonstrated in Fig. 2 and Fig. 3 using present theory and CPT. Since the transverse shear deformation effects of plate are not considered in the CPT, the values of nondimensional critical buckling load predicted by CPT are independent of thick-

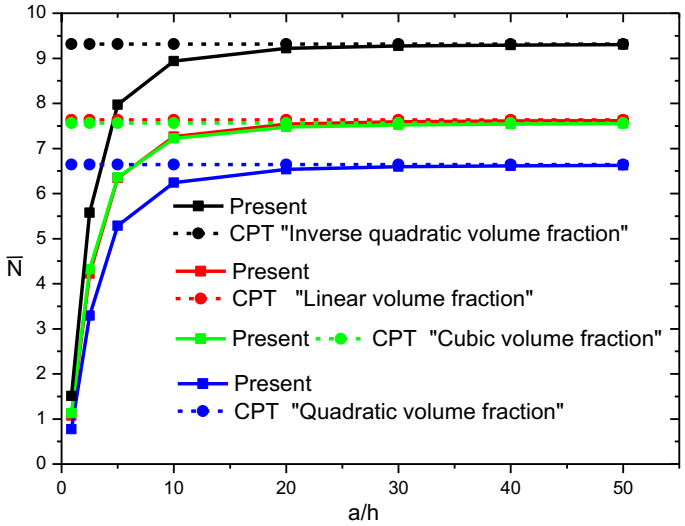

Fig. 2: The effect of thickness ratio on nondimensional critical buckling load $\bar{N}$ of simply supported square FGM plate under uniaxial compression along the x-axis (different volume fraction, $p = 2$, $\gamma_1 = -1$, $\gamma_2 = 0$).

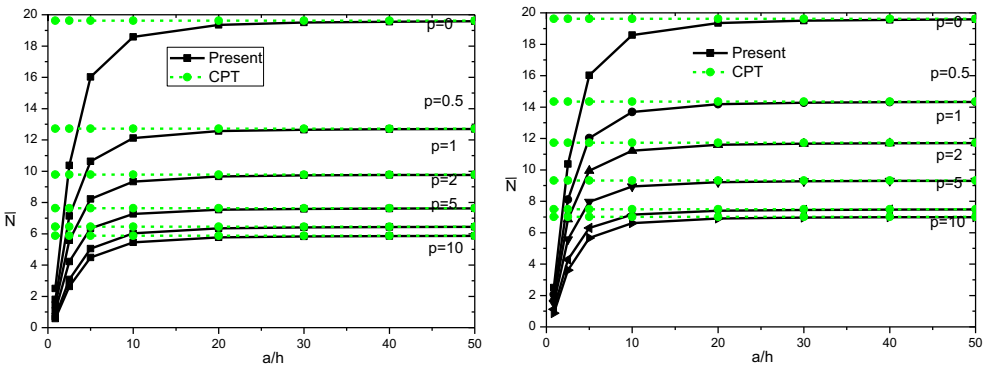

(a) (b)

Fig. 3: The effect of thickness ratio on nondimensional critical buckling load $\bar{N}$ of simply supported square FGM plate under uniaxial compression along the x-axis: (a) linear volume fraction; (b) inverse quadratic volume fraction, $\gamma_1 = -1$, $\gamma_2 = 0$.

ness ratio. Whereas, the values of nondimensional critical buckling load predicted by the present theory, which accounts for the transverse shear deformation effects, are dependent of thickness ratio. It is observed that the nondimensional critical buckling

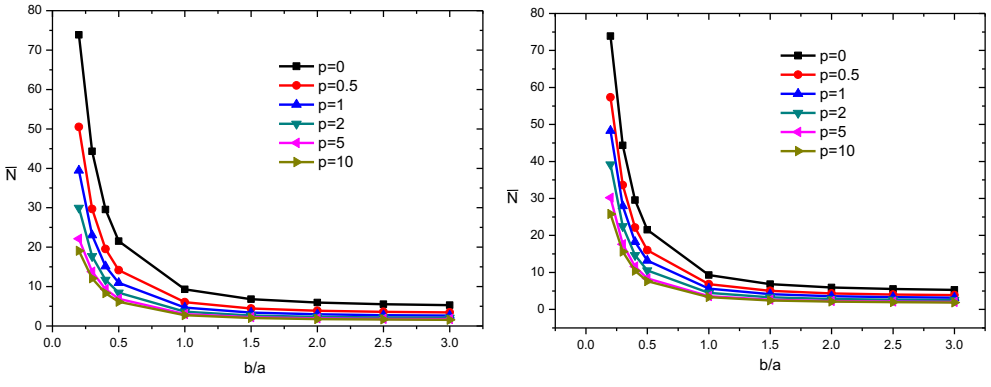

(a) (b)

Fig. 4: The effect of aspect ratio on nondimensional critical buckling load $\bar{N}$ of simply supported rectangular FGM plate ($a = 10h$) under biaxial compression: (a) linear volume fraction; (b) inverse quadratic volume fraction, $\gamma_1 = -1$, $\gamma_2 = -1$).

load increases by the increase of thickness ratio a/h, while the CPT overestimates the nondimensional critical buckling load of FG plate. The difference between two theories is considerable for thick plates ($a/h < 10$), and negligible for thin plates.

The effects of aspect ratio b/a on nondimensional critical buckling load of simple supported plate under biaxial compression are shown in Fig. 4. The thickness ratio a/h is assumed to be 10. It is shown that the nondimensional critical buckling load

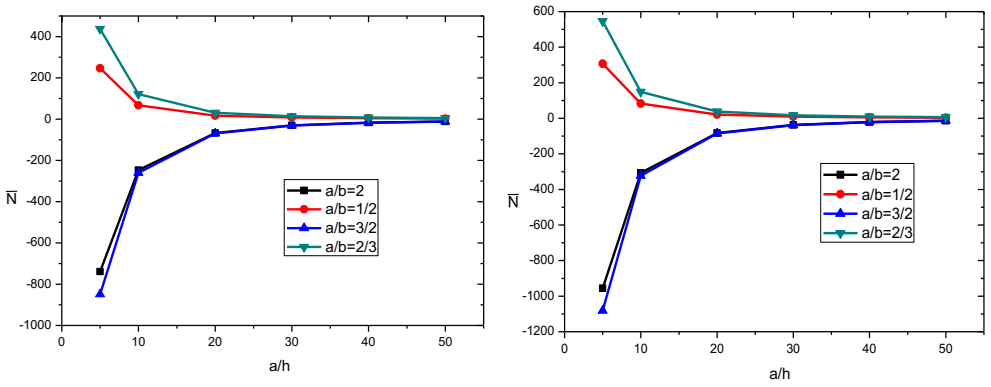

(a) (b)

Fig. 5: Critical buckling load of simply supported Al/Al_2O_3 plate ($p = 2$: (a) linear volume fraction; (b) inverse quadratic volume fraction, $\gamma_1 = -1$, $\gamma_2 = 1$) with variation of thickness ratio (a/h) and the aspect ratio b/a.

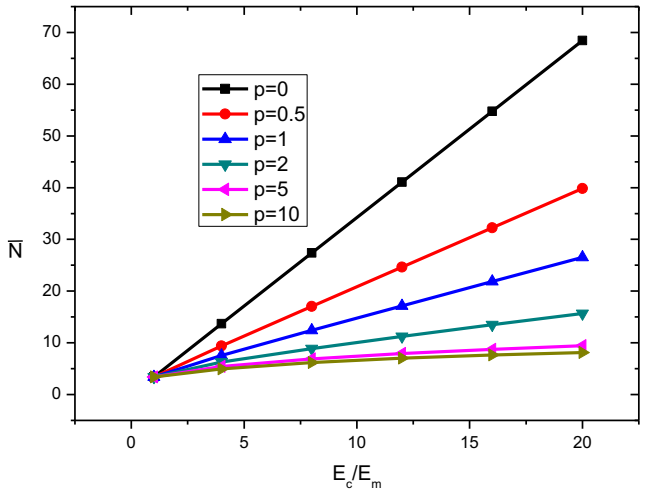

Fig. 6: The effect of modulus ratio on nondimensional critical buckling load $\bar{N}$ of simply supported square (Al/Al$_2$O$_3$) plate ($a = b = 10h$, $\gamma_1 = -1$, $\gamma_2 = 0$).

generally decreases by the increase of the aspect ratio b/a. The variation of nondimensional critical buckling load of plate versus thickness ratio a/h and the aspect ratio b/a is demonstrated in Fig. 5 using the present theory.

The variation of nondimensional critical buckling load of square plate versus the modulus ratio E_c/E_m of FGM for different values of power law index is demon-

Table 3: Nondimensional critical buckling load $\bar{N}$ of simply supported square FGM (Al/Al$_2$O$_3$) plate subjected to biaxial compression

a/h	Theory	volume fraction indexes (p)						
		0	0.5	1	2	10	20	100
10	Thai & Choi [29]	9.289	6.061	4.669	3.631	2.726	2.417	1.909
	Hao Zuo et al. [30]	9.153	5.988	4.640	3.638	2.736	2.405	1.883
	Present	9.289	6.061	4.669	3.631	2.726	2.417	1.909
20	Thai & Choi [29]	9.676	6.283	4.833	3.768	2.883	2.549	1.996
	Hao Zuo et al. [30]	9.638	6.255	4.811	3.752	2.879	2.543	1.988
	Present	9.676	6.283	4.833	3.768	2.883	2.549	1.996
100	Thai & Choi [29]	9.807	6.357	4.888	3.814	2.937	2.594	2.025
	Hao Zuo et al. [30]	9.806	6.358	4.889	3.815	2.938	2.594	2.025
	Present	9.807	6.357	4.888	3.814	2.937	2.594	2.025

strated in Fig. 6. It can be seen that the nondimensional critical buckling load increases as the ceramic -to- metal modulus ratio increases and decreases as the power law index increases.

Table 3 shows the comparisons of the nondimensional critical buckling loads $\bar{N}$ of simply supported square FGM (Al/Al_2O_3) plate subjected to biaxial compression obtained by the present theory with those given by Thai and Choi [29] and Hao Zuo et al. [30]. It can be seen that the results of present theory are in excellent agreement with those obtained by [29] for all values of thickness ratio a/h.

4 Conclusions

A new refined shear deformation theory (RTSDT) is developed for the buckling analysis of functionally graded plates (Al/Al_2O_3).

The mixture of the metal and ceramic with continuously varying volume fraction can eliminate interface problems of sandwich structures.

The volume fraction plays important roles in predicting critical buckling load of FG plates.

The values of nondimensional critical buckling load predicted by the present theory, which accounts for the transverse shear deformation effects, are dependent of thickness ratio.

The nondimensional critical buckling load increases by the increase of thickness ratio, while the CPT overestimates the nondimensional critical buckling load of FG plate. The difference between two theories is negligible for thin plates, and considerable for thick plates.

The number of primary variables in this theory is even less than that of first- and higher-order shear deformation plate theories, and moreover, it obviates the need for a shear correction factor.

All comparison studies demonstrated that the critical buckling loads obtained using the present refined theory (with four unknowns) and other higher-order shear deformation theories (with five unknowns) are almost identical.

Hence, it can be said that the proposed refined plate theory is accurate and simple in solving the buckling behaviour of FG plates.

References

[1] M. Koizumi (1997) FGM activities in Japan. *Composites Part B: Engineering* **28** 1-4.

[2] E. Reissner (1945) The effect of transverse shear deformation on the bending of elastic plates. *Journal of Applied Mechanics* **12** Trans. A69-A77.

[3] R.D. Mindlin (1951) Influence of rotatory inertia and shear on flexural vibrations of isotropic elastic plates. *Journal of Applied Mechanics* **73** 31-38.

[4] H. MATASUNAGA (2008) Analysis of functionally graded plates. *Composite Structures* **82** 499-512.

[5] R.B. NELSON, D.R. LARCH (1974) A refined theory of laminated orthotropic plates. *Journal of Applied Mechanics* **41** 177-183.

[6] E. REISSNER (1975) On transverse bending of plates including the effect of transverse shear deformation. *International Journal of Solids and Structures* **11** 569-573.

[7] K.H. LO, R.M. CHRISTENSEN, E.M. WU (1977) A high-order theory of plate deformation – part I: homogeneous plates. *Journal of Applied Mechanics* **44** 663-668.

[8] J.N. REDDY (1984) A simple higher-order theory for laminated composite plates. *Journal of Applied Mechanics* **51** 745-752.

[9] S.J. SINGH, S.P. HARSHA (2019) Buckling analysis of FGM plates under uniform, linear and non-linear in-plane loading. *Journal of Mechanical Science and Technolog* **33** 1761-1767.

[10] R.P. SHIMPI (2002) Refined plate theory and its variants. *AIAA Journal* **40**(1) 137-146.

[11] S.A. AMBARTSUMIAN (1958) On theory of bending plates. *Izv Otd Tech AN Nauk SSSR* **5** 69-77.

[12] M. KARAMA, K.S. AFAQ, S. MISTOU (2003) Mechanical behavior of laminated composite beam by the new multilayered laminated composite structures model with transverse shear stress continuity. *International Journal of Solids and Structures* **40**(6) 1525-1546.

[13] M. AYDOGDU (2009) A new shear deformation theory for laminated composite plates. *Composite Structures* **89** 94-101.

[14] Z. KACZKOWSKI (1968) "Plates. Statistical Calculations". Arkady: Warsaw.

[15] V. PANC (1975) "Theories of elastic plates". Prague: Academia.

[16] A. TOUNSI, M.S.A. HOUARI, S. BENYOUCEF, AND AL (2013) A refined trigonometric shear deformation theory for thermoelastic bending of functionally graded sandwich plates. *Aerospace Science and Technology* **24** 209-220.

[17] B. BOUDERBA, M.S.A. HOUARI, A. TOUNSI (2013) Thermomechanical bending response of FGM thick plates resting on Winkler-Pasternak elastic foundations. *Steel and Composite Structures* **14**(1) 85-104.

[18] M. LEVINSON (1980) An accurate simple theory of the statics and dynamics of elastic plates. *Mechanics Research Communications* **7** 343-350.

[19] M.V. MURTHY (1981) An improved transverse shear deformation theory for laminated anisotropic plates. *NASA Technical Paper* 1903.

[20] J.N. REDDY, C.F. LIU (1985) A higher-order shear deformation theory of laminated elastic shells. *International Journal of Engineering Science* **23** 319-330.

[21] M. SOBHY (2016) An accurate shear deformation theory for vibration and buckling of FGM sandwich plates in hygrothermal environment. *International Journal of Mechanical Sciences* **110** 62-77.

[22] M. TOURATIER (1991) An efficient standard plate theory. *International Journal of Engineering Science* **29**(8) 901-916.

[23] K.P. SOLDATOS (1992) A transverse shear deformation theory for homogeneous monoclinic plates. *Acta Mechanica* **94** 195-220.

[24] S. PITAKTHAPANAPHONG, E.P. BUSSO (2002) Self-consistent elasto-plastic stress solutions for functionally graded material systems subjected to thermal transients, *Journal of the Mechanics and Physics of Solids* **50**(4) 695-716.

[25] R. JAVAHERI, M.R. ESLAMI (2002) Buckling of functionally graded plates under in-plane compressive loading. *Journal of Applied Mathematics and Mechanics*. **82**(4) 277-283.

[26] B.A.S. SHARIAT, M.R. ESLAMI (2005) Buckling of functionally graded plates under in plane compressive loading based on the first order plate theory. In: *Proceedings of the Fifth International Conference on Composite Science and Technology*, American University of Sharjah, United Arab Emirates, pp. 161-166.

[27] M. BODAGHI, A.R. SAIDI (2010) Levy-type solution for buckling analysis of thick functionally graded rectangular plates based on the higher-order shear deformation plate theory, *Applied Mathematical Modelling* **34**(11) 3659-3673.

[28] H-T. THAI, D.H. CHOI (2012) An efficient and simple refined theory for buckling analysis of functionally graded plates. *Applied Mathematical Modelling* **36** 1008-1022.

[29] H.-T. THAI, D.-H. CHOI (2013) A simple first-order shear deformation theory for the bending and free vibration analysis of functionally graded plates. *Composite Structures* **101** 332-340.

[30] H. ZUO, Z. YANG, X. CHEN, Y. XIE, X. ZHANG (2014) Bending, Free Vibration and Buckling Analysis of Functionally Graded Plates via Wavelet Finite Element Method. *Computers, Materials & Continua* **44**(3) 167-204.